1 We thank all 3 reviewers for their positive and constructive comments. We address their specific
2 points below:

3 ***Anonymous - reviewer 3***

4 *General comments*

5 *This paper reports on a near surface profiler for sampling biogeochemical properties of seawater near*
6 *the surface, where important biological and air-sea exchange processes take place, and where*
7 *vertical characterization has proved difficult. The motivation in developing this profiling device would*
8 *be to study the effect of stratification on the biogeochemistry at the air-sea interface. There is no*
9 *doubt that the authors have invested tremendous effort in developing and deploying the NSOP.*
10 *However, I am a little disappointed with the scientific conclusions. In fact the article appears to be*
11 *more of a technical description of an instrument, and therefore I think it might have been more*
12 *appropriate for a more technical journal such as Methods in Oceanography. Therefore if the authors*
13 *wish to publish this in OS, I suggest that they provide some further material on the scientific*
14 *consequences of the NSOP. I do not think that this will require much effort, and although my major*
15 *revisions rating appear to be a little severe, I do not think it will require much effort. The current effort*
16 *in their conclusions - "The presence or absence of chemical and biological gradients within near*
17 *surface stratified layers has been difficult to assess. NSOP is a platform with the capability to*
18 *successfully resolve gradients in these near surface layers." - is weak, and I have no doubt that given*
19 *the list of authors here, a little more effort would provide much improved conclusions. For example:*
20 *how well does the temperature-pCO2 relationship of 4.23% per degC hold? What are the global*
21 *consequences for stratification on air-sea gas exchange?*

22 We respectfully disagree with the reviewer. There is plenty of evidence of method-driven papers in
23 Ocean Sciences (e.g. Saltzman et.al 2009, Hemming et.al 2017, Schneider-Zapp et.al 2014 and
24 Arévalo-Martínez et.al 2013). A more detailed description of scientific results based on 4 cruises and
25 a seasonal study is planned as a later publication, which will include discussions on the
26 temperature/CO_2 relationship and global fluxes. However, we agree that some of the results
27 presented here can be discussed in more detail. To demonstrate how NSOP profiles may influence
28 air/sea fluxes we have calculated how the fluxes change using the near-surface concentrations. We
29 have added the following paragraph:

30 *We have adjusted the second paragraph of our conclusions (P20, L17):*

31 'Near surface stratification in the upper few metres of the ocean due to temperature and salinity
32 gradients is a well-documented phenomenon. The presence or absence of chemical and biological
33 gradients within near surface stratified layers has been difficult to assess. NSOP is a platform with the
34 capability to successfully resolve gradients in these near surface layers. The data presented in this
35 paper demonstrate that near surface gradients in trace gases can lead to substantially different
36 fluxes depending upon the seawater depth that is used to calculate the flux. Assuming that the effect
37 of temperature and salinity gradients on the flux can be accounted for using remote sensing methods
38 (e.g. Shutler et.al 2016), then the change in flux is directly proportional to the change in ΔC. In the
39 case of the coastal DMS profile, a higher concentration (2.58±0.02 nM) was observed 0.5 m below
40 the sea surface compared to concentrations at 5 m (2.36±0.03 nM). Assuming that the atmospheric

1 concentration of DMS was negligible(a typical approach for DMS fluxes, see Lana et al., 2011),
2 computing the flux with the 5 m waterside concentration instead of the 0. 5m waterside
3 concentration means the flux is underestimated by 9.3%. . In the case of the Celtic Sea CO_2 profile,
4 the concentration at 0.5 m (389.60 ±0.36 µatm) was higher than at 5 m (385.92 ±0.36 µatm). The
5 atmospheric CO_2 concentration was 398.1 ±0.3 µatm, which means that the surface water was less
6 undersaturated than implied by the seawater concentration at 5 m. Using the 5 m waterside CO_2
7 concentration leads to an overestimation of the ΔC and flux by 43.5% compared to using the 0.5 m
8 waterside CO_2 concentration. The magnitudes of these concentration gradients are significant.
9 However, such gradients (in magnitude and direction) do not persist for all hours of the day, under
10 different environmental conditions and in all regions of the global ocean. A subsequent publication
11 will discuss NSOP data collected during four cruises as well as the wider prevalence and implications
12 of near surface CO_2 gradients.'

13

14 ***Maria Ribas Ribas – Reviewer 1***

15 General comments

16 *The present paper under review for Ocean Science describes state-of-the-art technology to measure*
17 *high resolution profile in the upper 5 m of the ocean. I appreciate the effort of research, develop and*
18 *validation of the authors. Everyone working on R&D knows that behind these two examples profiles*
19 *are a lot of trial-error and frustration. I also think the described technology fill a gap and it is really*
20 *important and that it is adequate to the scope of the journal. I will recommend publication after some*
21 *minor/moderate revision. I hope the comments help to improve the ms. I understand first author is*
22 *PhD student and I congratulate him for the nice work .*

23 *Specific comments*

24 *Page 4-line 15 Define ID-*

25 As this is the only occurrence of ID, we have changed ID to inner diameter

26   *4-25 I am curious to know what the maximum wave height is and wind you deploy. Also applicable*
27 *for my first comments on real live application.*

28 This information is already in the text on Pg 5 L 21-23

29 *5-4 What is the maximum distance?*

30 In this case the maximum extended length of the crane arm was ~7m. Pg 5 L 3-4 changed to

31 "through a block on a fully extended crane arm of 7m to maintain this distance between NSOP and
32 the ship."

33 *5-12 unfortunately I can't access to supplement material. I would love to see the videos*

34   *5-22 What is the limitation of the deployment length? Battery? Can other deployments, ship*
35 *operations happen at the same time, like CTD, so you have a concurrence profiles?*

1   The information on the maximum deployment length is already in the manuscript on Pg 6 L 12-15.

2   The fact that no other instrumentation can be deployed simultaneously is a pertinent point. Pg 4 L 28

3   changed to "NSOP was always deployed while the ship was on station and not at the same time as

4   other overboard deployments."

5   *6-10 Please check figure order of appearance, suddenly here we found Fig. 9.*

6   Reference has been removed and a reference to this part of the text has been included in the caption

7   of figure 9.

8   *7-21 In text and figure, unify use of litre with capital L*

9   All instances have been changed .

10 *7-29 How was the pressure inside the equilibrator measured?*

11 All pressure measurements were made with the Licor analyser, in close proximity to the equilibrator.

12 Unfortunately there is no way to measure the pressure internally without compromising the

13 membrane. We are confident that the equilibrator pressure is 0.4 kpa above ambient. Changed p7 L

14 26 to 'The continuous gas flow through the system caused a small 0.4 kPa pressure increase in the

15 Licor measurement cell, this was in good agreement with a similar observation by Burke Hales

16 (0.5kpa > ambient pressure; Personal communication).'

17 *9-1:4 Could you provide more details of the membrane (µm...) –*

18 The membrane material, total surface area and internal liquid and gas side volumes are now

19 included. Pg 9 L 1 change to "We used a polypropylene membrane equilibrator (Liqui-Cel, model

20 2.5x8) with liquid and gas volumes of 0.4 L and 0.15 L and a surface area of 1.4 m^2. Due to its large

21 surface area to volume ratio and membrane porosity (50%), the Liqui-Cel expedites gas transfer and

22 efficiently achieves equilibration"

23 *Figure 3 caption: Could you add legend (nice to understand the figure without the need to read first).*

24 *What is LPM in the x-axis?-*

25 Legends are discouraged by the ocean science journal. LPM has been changed to L min^{-1} and ml

26 changed to mL throughout.

27 *10-16 what is m/z –*

28 Mass is now defined as m and charge as z.

29 *10-19: two points in the reference 11-12: wrong use of () in the reference –*

30 This has been corrected.

31 *Figure 4: what is the magnitude of the change? For example from 400 to 1000 ppm or 400 to 450*

32 *ppm (that will make a different, right?)? –*

1 The change was from 350 to 400 ppm for CO_2 and 0 to 2 nmol L^{-1} for DMS. The absolute magnitude of
2 the change does not matter for the calculation of response time so long as the change is large
3 enough to be clearly detected by the instrument.

4 *I miss a table of comparison of discrete and continuous operation. Also another one of the sensor use*
5 *with the accuracy/frequencies... to have a quick overlook of the system. –*

6 The two modes of deployment are not directly comparable and there is insufficient information to
7 justify a table.

8 *12-23 Probably not need to say the SOP# -*

9 We feel it is helpful to retain the reference to the SOP as the document is ~200 pages.

10 *In all figures, A), B) C) in the figures are capital but in the captions are not. Please unify.*

11 The capitalisation in the figures has been changed.

12 *14-13 How much of the unsaturated?*

13 The atmospheric CO_2 concentration is now included. P14 L 13 changed to 'Seawater temperature was
14 16.61± 0.06 °C. At 14:20 hrs (UTC) $fCO_{2(atm)}$ was 398 µatm and$fCO_{2(sw)}$ was 389 µatm at 0.67 m
15 meaning the ocean was undersaturated with respect to the atmosphere. The temperature and
16 seawater CO_2 were the expected magnitude for summer in the Celtic Sea (Frankignoulle and Borges,
17 2001).'

18 *15-15 Could you provide a bit more detail about this mooring? Maybe a map with location site and*
19 *the mooring will be helpful for readers not familiar with the area.*

20 A map of both deployment sites in now in the supplement. Additional information about the mooring
21 can be found in the cruise report
22 https://www.bodc.ac.uk/resources/inventories/cruise_inventory/reports/dy033.pdf .P15 L15
23 changed to 'We compare the NSOP temperature profile with thermistor readings from a series of
24 Sea-Bird Scientific (SBE 56) sensors (0.3, 0.6, 1.5, 3.5 and 7 m depth) mounted on a nearby
25 temperature chain moored ~2.8 km away (49.403°N, -8.606°E) from the deployment site'.

26 *Figure 6 and 9 are quite confusing, as depth is plot with time instead as usual oceanography profile*
27 *way. In a related note, what is the different info from figure 9 and 10?*

28 These plots demonstrate that the data is collected continuously at high frequency rather than
29 discrete samples. We have shown the time series data here as high frequency seawater pCO_2 data is
30 rarely presented, so showing how this varies is important. In addition, this paper focuses on a new
31 method and we want to be absolutely clear of the data processing steps that are required rather
32 than 'rush to the final plot'.

33 *16-1:6 Can the drifting from ship cause turbulence/mixing? Would be possible to measure turbulence*
34 *within the NSOP?*

1 NSOP may create a small amount of local turbulence but we did not see any evidence of this in our
2 profiles. It would be possible to measure turbulence from NSOP and we have added turbulence
3 sensors to the list of possible additional sensors on P 19 L 9.

4 *17-2 When you talk about significantly different I expect a statistical test.*

5 As the errors on the CO_2 measured by NSOP and the underway system are two standard errors, the
6 fact they don't overlap indicates they are statistically different at the 95% confidence interval. To be
7 absolutely clear, P17 L2 has been changed to 'A paired t-test showed that thefCO$_2$ measured in the
8 surface bins on the downcast and upcast are were significantly different (p = <0.001) .'

9 *17-1:5 This paragraph is really important and key message of paper so I will like to have more*
10 *discussion on it. What is the role of sea surface microlayer?*

11 The sea surface microlayer was not discussed in detail as it could not be sampled with NSOP, we
12 agree that it should be mentioned. P 17 L1 Added 'Trace gas concentrations may also be different in
13 the sea surface microlayer but sampling that close to the surface is beyond the capabilities of NSOP.
14 Complimentary measurements of the sea surface microlayer could be made using other state of the
15 art purpose built sampling platforms such as the Sea Surface Scanner (Ribas –Ribas et.al., 2017).'

16 *What is the implication of the calculations of flux as normally do it from 5 m? ...*

17 *Refer to our response to anonymous reviewer 3.*

18 *17-18:19 This comparison with underway CO2 is also really important. Can you provide more detail? I*
19 *will think that ship disturbance will have more influence of underway system... What is RMS? Why we*
20 *should care about NSOP if they give similar results of usual pCO2 instrument? I really think it is*
21 *important, do not take me wrong, I just think a bit more discussion will be good*

22 The original manuscript was unclear so we have improved the wording:

23 We have changed P17 L 18 to:- 'However during a deployment on the 19th July 2015, the fCO$_{2(sw)}$
24 measured by NSOP at 5 m agreed well with independent measurements from the underway system,
25 difference = 1.7+/- 4.18 µatm,). The agreement between the two systems is in line with previous
26 intercomparisons (Kortzinger 2000; Ribas-Ribas 2014).

27

28 <u>***Anonymous – reviewer 2***</u>

29 *General comments*

30 *The authors presented a new sampling technique to sample and measure the vertical profiles of*
31 *physical and chemical parameters in the subsurface layer of the ocean (<10 m). This indeed improves*
32 *the very surface layer sampling for chemical tracers. The paper is overall well written with the*
33 *exception of a few confusing sentences. Some of the figures present redundant information, and*
34 *could be removed. However, the main problem of the paper, I feel, is lack of discussion on how the*
35 *whole technique may impact the estimation of air-sea exchange. Does it really matter that we need*
36 *to sample the very subsurface layer (e.g.,∼1m) of the seawater to obtain a very accurate flux*

1   estimate? Or it may be good enough to sample 4m below the sea surface as the traditional sampling

2   system?

3   In response to a similar comment from Reviewer 3, we have added a paragraph on this subject.

4   *Specific comments*

5   *Pg2, lines 22 – 30: Authors discussed near surface stratification due to certain physical processes*

6   *here. It is worth to note and mention that, people have been using CFC-11 to correct physical effect*

7   *on estimated air-sea fluxes (see Lobert et al., 1995; Butler et al., 2016; Yvon-lewis et al., 2004; Hu et*

8   *al., 2013).*

9   This section discusses the calculation of air/sea flux using estimates of gas transfer velocity combined

10   with global databases of trace gas concentrations. This approach to calculating air/sea flux is

11   commonly-used in Earth System models. Near surface gradients may impact upon the calculation of

12   air/sea fluxes.

13   We are not claiming that other approaches (such as the use of CFCs, which incorporate the implicit

14   effects of physical forcing on gas exchange) would be influenced by near surface gradients. However,

15   discussing the CFC method would be a deviation from the narrative of the text so we have not added

16   anything to this effect.

17   *Pg12, lines 7 – 9: "The delay between a bucket switch and CO2 change in the Licor was timed at*

18   *138s...". This is confusing. Does this delay include CO2 response time in the equilibrator and the time*

19   *from sampling to the equilibrator? If it is, define it. Also, this sentence seems out of place here.*

20   P12 L7 We have changed the wording and structure of this section to improve clarity:

21   'We used different approaches to assess the delay between instantaneous miniCTD measurements

22   and water arriving to the ship for analysis. The delay between seawater entering the inlet and

23   reaching the equilibrator was calculated as 114 s using the internal volume of NSOP tubing (0.5 in ID,

24   54 m length) and a seawater flow rate of 4.15 L min^{-1}.Delay correlation analysis between the NSOP

25   miniCTD temperature sensor and a second sensor positioned at the entrance to the equilibrator gives

26   a similar delay of 112 s. Note that the total delay of the system is greater because it also includes the

27   time that equilibrated gas takes to reach the Licor. We determined the total delay by moving the

28   seawater inlet quickly between two buckets with distinctly different CO_2 concentrations and timing

29   how long it took for the signal to be detected by the Licor (139 s; Fig. 4).'

30

31   *Pg12, lines 21 – 25: list equations to be clearer.*

32   The equations are commonly used by the community and are well detailed in (Dickson 2007). We

33   feel this is sufficient.

34   *Pg 12, lines 26 – 28: redundant information.*

1   Removed

2 *Fig. 5: I don't think this figure provides extra information or value other than the sentence described*
3 *in Pg 11, line21. So, you may consider remove it.*

4 The reference to this figure remains in the text but the figure has now been moved to the
5 supplement.

6 *Figs. 6 & 7: Redundant. Recommend to remove fig. 6. Figs. 9 and 10: redundant information.*
7 *Consider remove fig. 9*

8 Please see earlier response to Ribas-Ribas.

9 *Also, fig. 7 looks a little messy with depth contours.*

10 The lines in Fig. 7c are not depth contours. They are a time series of temperature for sensors at
11 different depths. We have added additional detail to the figure legend to clarify this.

12 *Pg. 16, line 18: Density was not used in the later discussion. I am not sure why you want to mention*
13 *and discuss density profiles here. Consider remove it from the text and figure.*

14 Density determines the stratification and is affected by both salinity and temperature. We think it is
15 necessary to include density as it is more useful to the reader than just plotting temperature.

16 *Pg. 17, lines 3 – 5: why do fco2 profiles show the largest difference in the surface, and not in the layer*
17 *where the temperature showed the largest difference (4.5 – 2 m below water)? The explanation given*
18 *by the authors is not convincing. Since the amount of co2 outgassing due to surface seawater*
19 *warming (during upcast) can be calculated using temperature, salinity and solution of CO2, it is not*
20 *hard to estimate how much the difference between down cast and up cast was due to physical effect,*
21 *and how much was due to biological influences.*

22 We are a bit confused by this comment. Figure 8 shows that there is a gradient in fCO_2 down to a
23 depth of 5 m. The temperature effect on fCO_2 is already accounted for - the profile we show is
24 seawater fCO_2 after correction for *in situ* temperature.

25 *Pg. 17, lines17–19: 3 uatm seems ahuge difference considering the variation off co2 observed in the*
26 *subsurface layer. Did the authors consider the different response time in two different equilibrators?*
27 *Why are their measured values so different?*

28 We apologise - our original text is misleading. We said that "CO_2 agrees to within 3 uatm" but the
29 mean difference is actually 1.7+/- 4.18 uatm. This is very similar to previous comparisons between
30 shower and membrane equilibrators (Hales et.al,. 2004). This is also close to the (Kortzinger et.al ,.
31 2000) comparison of 1 uatm, which used very similar equilibrator setups. As detailed in our response
32 to reviewer Ribas-Ribas, we have changed the paragraph on P17, L 17-19 to make this clearer. Also,
33 note that we do consider the response time in the equilibrators (see text on P10, L1-14).

34 *Pg. 18, lines 15 – 16: confusing. To me, the increased fluorescence is likely due to phytoplankton*
35 *located at the bottom or below the subsurface layer. –*

1 We disagree. It is well established that phytoplankton fluorescence becomes quenched in the very
2 near surface layers and does not suggest a change in phytoplankton concentration with depth. (Serra
3 et.al 2007, Gibb et.al 2000 and Smyth et.al 2004).

4

5

6

A measurement system for vertical seawater profiles close to the air/sea interface

Richard P. Sims[1,2], Ute. Schuster[2], Andrew. J. Watson[2], Ming Xi. Yang[1], Frances. E. Hopkins[1], John. Stephens[1] and Thomas. G. Bell[1,*]

[1]{Plymouth Marine Laboratory, Plymouth, United Kingdom}

[2]{University of Exeter, Exeter, United Kingdom}

Correspondence to: T. Bell (tbe@pml.ac.uk)

Abstract

This paper describes a Near Surface Ocean Profiler, which has been designed to precisely measure vertical gradients in the top 10 m of the ocean. Variations in the depth of seawater collection are minimised when using the profiler compared to conventional CTD/rosette deployments. The profiler consists of a remotely operated winch mounted on a tethered yet free floating buoy, which is used to raise and lower a small frame housing sensors and inlet tubing. Seawater at the inlet depth is pumped back to the ship for analysis. The profiler can be used to make continuous vertical profiles or to target a series of discrete depths. The profiler has been successfully deployed during wind speeds up to 10 m s^{-1} and significant wave heights up to 2 m. We demonstrate the potential of the profiler by presenting measured vertical profiles of the trace gases carbon dioxide and dimethylsulfide. Trace gas measurements use an efficient microporous membrane equilibrator to minimise the system

8

1 response time. The example profiles show vertical gradients in the upper 5 m for temperature,

2 carbon dioxide and dimethylsulfide of 0.15 °C, 4 μatm and 0.4 nM respectively.

3

1   Introduction

5 Exchange between the ocean and atmosphere is an important process for many gases.

6 Important examples include carbon dioxide (CO_2), for which the oceans account for 25% of

7 the sink for anthropogenic emissions (Le Quéré et al., 2016), and dimethylsulfide (DMS),

8 which has an oceanic source and influences cloud properties with implications for the global

9 energy balance (Quinn and Bates, 2011). The magnitude and direction of air/sea gas transfer

10 is typically represented by Flux=$K\Delta C$ (Liss and Slater, 1974), where ΔC is the concentration

11 difference across the air-sea interface and K is the gas transfer velocity. Direct flux

12 measurements (Bell et al., 2013; Yang et al., 2013; Miller et al., 2010) are only possible for a

13 small number of gases and are not made routinely. Most flux estimates use a wind speed-

14 based parameterisation of K (e.g. Wanninkhof, 2014) coupled with measurements of ΔC.

15 CO_2 is the most well-observed trace gas in the surface ocean, with 14.5 million measurements

16 compiled into a global database, the Surface Ocean CO_2 Atlas (SOCAT),

17 http://www.socat.info/ (Bakker et al., 2016). Global trace gas databases also exist for gases

18 such as methane and nitrous oxide https://memento.geomar.de/ (Bange et al., 2009),

19 dimethylsulfide http://saga.pmel.noaa.gov/dms/ (Lana et al., 2011) and halocarbons

20 https://halocat.geomar.de/ (Ziska et al., 2013). Accurate estimation of air/sea flux requires

21 concentration measurements that are representative of the interfacial concentration difference.

22 Surface seawater samples are often collected from the underway seawater intake of research

23 vessels, typically at 5-7 m depth. A source of potential error in air/sea flux calculations arises

24 from the assumption of vertical homogeneity within the mixed layer (Robertson and Watson,

25 1992). If vertical concentration gradients exist in the mixed layer, then underway seawater is

26 not representative of the interfacial layer, which could create a global sampling bias (McNeil

27 and Merlivat, 1996).

28 Vertical gradients in trace gas concentrations have been observed under conditions that are

29 favourable for near surface stratification (Royer et al., 2016). At low wind speeds, high solar

30 irradiance can suppress the depth of shear-induced mixing to create a near surface layer

31 several degrees warmer than the water below (Ward et al., 2004; Fairall et al., 1996). Near

32 surface stratification in the marine environment can also be induced by freshwater inputs such

9

1   as rain (Turk et al., 2010) and riverine discharge. Changes in surface seawater temperature

2   and salinity alter the solubility of dissolved gases and thus the amount available for air/sea

3   exchange (Woolf et al., 2016). Dissolved gases isolated in the upper few metres of the ocean

4   may additionally be modified by physical process such as air/sea exchange and

5   photochemistry. Marine biota confined within the stratified layer (Durham et al., 2009), may

6   also alter trace gas concentrations. For the purposes of this paper, near surface gradients are

7   defined as physical and/or chemical gradients in the upper 10 m of the ocean.

8   Identifying and quantifying near surface gradients in trace gas concentrations is challenging.

9   Ship motion often inhibits near surface measurements made with the standard oceanographic

10   approach of sampling with Niskin bottles mounted on a CTD rosette. Substantial vertical

11   movement of the rosette limits how close to the surface a sample can be taken. For example, a

12   crane arm 4 m above the sea surface and 11 m from the centreline of a ship that is rolling by

13   ±4 degrees will induce ~1.5 m sample depth variation every few seconds. CTD/Niskin bottle

14   sampling requires that the rosette is kept below the sea surface. Sampling within 2 m of the

15   sea surface is often impossible, even under relatively calm conditions.

16   We present a Near Surface Ocean Profiling buoy (NSOP) designed for measuring near surface

17   profiles. The design principles for NSOP were:

18   (1) Platform diameter less than the wavelength of most open ocean waves, allowing it to ride

19   the swell;

20   (2) Short sampling arm close to the sea surface to reduce vertical movements induced by

21   platform motion;

22   (3) Capable of deployment close to the ship (to retrieve water for trace gas analysis), but away

23   from major turbulence and motion due to the ship itself.

24   Example profiles from a cruise on the European continental shelf (*RRS Discovery*, DY033,

25   July 2015) and in the English Channel on board the *RV Plymouth Quest* (part of the Western

26   Channel Observatory, Smyth et al., 2010, April 2014) are discussed.

27

1 ## 2 Methods

2 ### 2.1 Near Surface Ocean Profiler (NSOP) description

3 NSOP is a repurposed ocean buoy (1.6 m diameter) with a central lifting eyelet (Fig. 1). The

4 top of the buoy is 0.5 m above the sea surface. Mounted on top of the buoy are a line of sight,

5 remotely operated winch (Warrior Winch, model C8000) and a gel battery (Haze, model

6 HZY-S112-230). The winch feeds Kevlar rope through a block and tackle with a 3:1 ratio to

7 reduce rope pay-out speed to ~0.05 m s^{-1}. The block and tackle is attached to the end of an

8 outstretched arm 0.25 m from the outer edge of the buoy. The winch line is attached to an

9 open frame (0.35 m diameter, 0.8 m height) with the capacity to house multiple sensors.

10 Desired sampling depth is targeted using knowledge of the winch pay-out speed. Rope pay-

11 out is then timed with a stopwatch. This approach only approximately regulates the sampling

12 depth because: (i) winch pay-out varies slightly depending on the amount of rope on the

13 spool; and (ii) variable horizontal current strength affects the vertical versus horizontal

14 position of the sampling frame. To minimise horizontal movement of the sampling frame we

15 attached a 10 kg weight to the base of the frame.

16 The primary sensor on the sampling frame is a small CTD (Valeport miniCTD) set to sample

17 at a high frequency (>1 Hz). Under calm conditions it is possible to sample as close as 0.1 m

18 from the air/sea interface when the miniCTD and tubing are mounted near the top of the

19 frame. Rougher conditions demand that the frame be kept deeper (~0.5 m) as motion can

20 momentarily bring the sensors and tubing out of the water. An emergency tag line was

21 attached to the sampling frame in case the winch line failed. Seawater for trace gas analysis

22 was pumped back to the ship at 3.5 L min^{-1} through a 50 m PVC hose (0.5 in ~~ID~~inner

23 diameter). A heavy duty peristaltic pump (Watson Marlow, model 701IB/R), primed with

24 water from the ships underway supply was used to overcome the large hydraulic head (~4 m).

25 The open end of the tubing was located at the same depth as the miniCTD. Water arriving to

26 the ship's laboratory was divided, with ~3.0 L min^{-1} for flow-through analysis (e.g.

27 equilibrator for trace gases) and ~0.5 L min^{-1} for discrete samples (e.g. total alkalinity).

28 We assessed the depth resolution capability of NSOP at a particular depth by looking at

29 pressure variations under calm conditions with a fixed amount of winch rope paid out. In calm

30 to moderate conditions (<2.5 m significant wave height) the amount of vertical movement

31 indicated by the standard deviation (SD) in the depth is ±0.18 m (~~see~~ Fig. ~~S2~~ S1,~~in~~

1 ~~Supplemental~~ supplementary information). During 4 deployments in rough conditions (>2.5

2 m significant wave height), the depth variability increased as the sampling frame was lowered

3 (at 5 m, SD was ±0.275 m).

2.2 NSOP deployment

5 On a large research vessel such as the *RRS Discovery*, the deployment and recovery of NSOP

6 requires close coordination between the bridge and 3 personnel on deck. NSOP was always

7 deployed while the ship was on station and not at the same time as other overboard

8 deployments. Ship orientation during deployments was typically with bow into the wind but

9 also accounted for swell and current direction/speed. NSOP was lifted by the aft crane (Fig.

10 1). Once NSOP was lowered to the surface it was detached from the crane via a quick release.

11 Two slack lines were looped through eyelets on the free-floating NSOP to maintain its

12 position close to the ship. A third slack line was connected to the top of the buoy and passed

13 through a block on a fully extended crane arm ~~to maintain distance (minimum 7 m)~~of 7 m to

14 maintain this distance between NSOP and the ship. The slack lines successfully inhibited the

15 tendency of NSOP to drift horizontally without disrupting its ability to ride the swell. The

16 instrument frame acted like a sea anchor and minimised rotation of NSOP. A 4 m lifting strop

17 used for recovery was connected to the lifting eyelet and loosely lashed to the aft slack line.

18 During retrieval, the slack lines were hauled in and the crane and jib arms brought towards the

19 ship to bring NSOP alongside. The lifting strop was then parted from the slack line and

20 attached to the crane to lift NSOP back on deck. For additional photographs of a NSOP

21 deployment ~~and~~ and videos of NSOP during a deployment and in operation~~,~~ see Fig. S2 and

22 videos, supplemental ~~material~~ry information.

23 Turbulence from the ship's propellers has the potential to mix the water column and destroy

24 any near surface gradients. The ship did not use the aft thrusters whenever conditions were

25 suitable (mild sea state, weak currents and no local hazards). Keeping NSOP away from the

26 ship limited disruption of near surface gradients by the thrusters and reduced the risk of line

27 entanglement in the aft propellers. Our winch did not have a groove bar to feed the rope onto

28 the winch drum, leading to an increased likelihood of snagging during spooling. To minimize

29 snagging, the rope was manually fed onto the winch spool before deployments. Visual

30 monitoring of the NSOP frame, slack lines and winch spool is important during deployment.

1   NSOP has been successfully deployed in 'moderate' sea states up to Beaufort force 5 (~10 m

2   s^{-1} wind speed and wave heights of ~2.0 m). Deployment length typically varied from 1-3
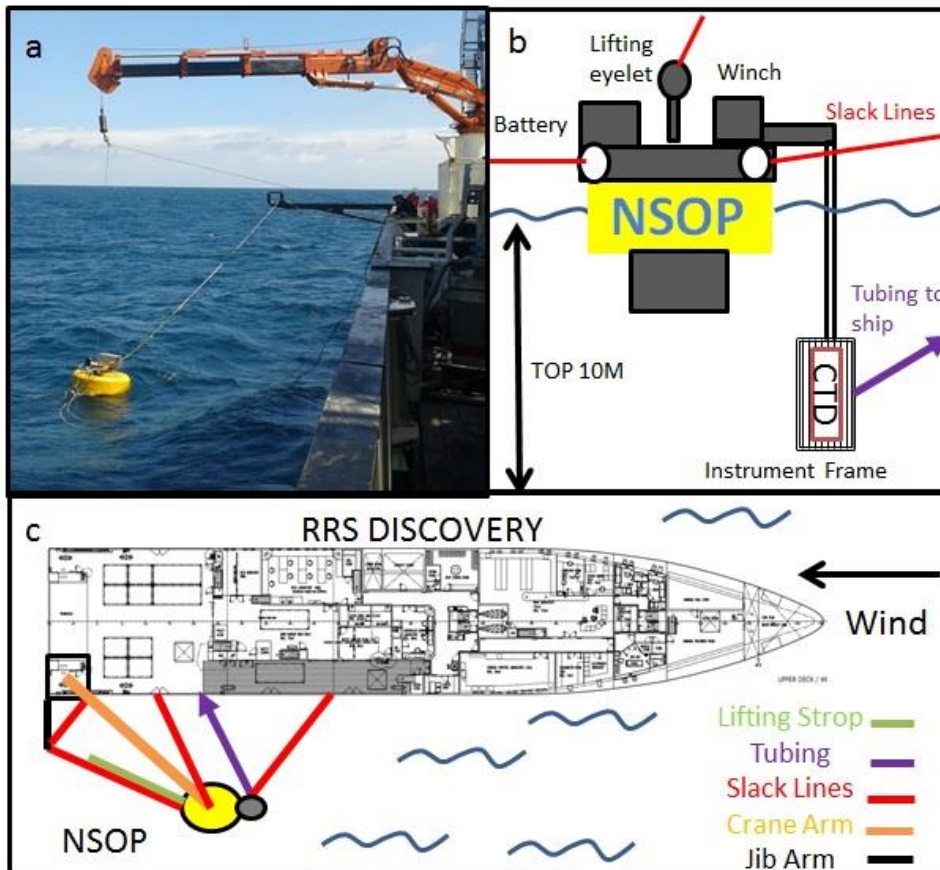
3   hours.

4

5

Figure 1: Different points of view of an NSOP deployment: (a) Image from a deployment on
RRS Discovery in May 2015 (Cruise DY030); (b) Schematic cross section of NSOP including
tubing back to ship (purple) and slack lines (red); and (c) Top down schematic from a research
ship including ship orientation. Not to scale.

10

11   NSOP can be used in two profiling modes: 'continuous' and 'discrete'. Continuous profiling

12   maximises vertical coverage and involves the winch continuously paying rope in and out at

13   ~0.05 m s^{-1}. A complete down/up profile to 10 m can be conducted in approximately 7 minn

14   (Fig. 9). Depth resolution during continuous profiling is determined by the measurement

15   response time. Instruments with rapid response times such as the miniCTD temperature and

13

1   conductivity sensors (0.15 s and 0.09 s) have theoretical depth resolutions of 0.75 cm and

2   0.45 cm respectively. Actual depth resolution will also be affected by the sampling depth

3   variability of the NSOP instrument frame. A measurement setup with a longer response time

4   (such as for seawater CO_2) requires a different approach (see Section 2.5).

5   During discrete profiling, the winch pays out a fixed amount of rope (typically 0.5 m) and the

6   sampling frame is left at a fixed depth. After a fixed sampling period, more rope is paid out.

7   The process is repeated down and then up such that a set of discrete depths are sampled in a

8   'stepped' profile. The discrete profiling depth resolution is determined by the depth

9   fluctuations when sampling at a fixed depth (see Section 2.1). Discrete profiles are a more

10 appropriate approach for measurement systems with a longer response time. A discrete profile

11 with 0.5 m steps down to 5 m and back to the surface using a 2.5 min sampling period takes

12 about an hour. The sampling period at each depth and frequency/distribution of depths within

13 the profile can be adjusted to suit sampling priorities.

14 The maximum deployment time is limited by the capacity of the winch battery. When under

15 no load, the battery allows for approximately 3 hours of operation in the continuous mode.

16 Discrete profiling requires substantially less winch usage such that battery drainage is even

17 less of a concern.

18 **2.3 CO_2 analysis**

19 The CO_2 measurement system (Fig. 2) is a modified version of the system described by

20 (Hales et al., 2004). Seawater from the NSOP inlet was passed through the equilibrator (see

21 Section 2.3.1) at ~3 L min^{-1} and the flow rate monitored (Cynergy ultrasonic flow meter,

22 model UF25B). A compressed nitrogen gas supply, maintained at a constant flow rate of 100

23 ~~ml~~ mL min^{-1} (Bronkhurst mass flow controller, model F-201-CV-100) flows through the

24 equilibrator in the opposite direction to the seawater flow. The gas has high water vapour

25 content after equilibration and is dried (Permapure nafion dryer, model MD-110-48S-4). The

26 dried sample then enters the analytical cell of a NDIR Licor 7000, which is protected with a

27 0.2 µm filter (Pall, Acro 50).

28 CO_2 measurements at atmospheric pressure as recommended by Dickson et al. (2007) were

29 not possible due to the nature of the experimental setup. The continuous gas flow through the

30 system caused a small 0.4 kPa pressure increase in the Licor measurement cell, this was in

31 good agreement with a similar observation by Burke Hales (0.5kpa > ambient pressure;

14

1 The elevated pressure was taken to be representative of the

2 equilibrator pressure and was used to obtain the partial pressure of CO_2 in the equilibrator

3 ($pCO_{2(eq)}$).

4 The Licor was calibrated using three CO_2 standard gases before and after each NSOP

5 deployment. The concentrations of the standard gases (BOC Ltd.) were determined by

6 referencing against US National Oceanic and Atmospheric Administration certified standards

7 (244.91, 388.62, 444.40 ppm) in the laboratory. The seawater temperature at the entry and

8 exit ports of the equilibrator was recorded at 1 Hz (Omega ultra-precise 1/10 DIN immersion

9 RTD) using stackable microcontrollers (Tinkerforge master brick 2.1 and PTC bricklet).

10 Equilibrator temperature probes and the miniCTD temperature sensor were calibrated before

11 and after each cruise against an accurate reference sensor (Fluke, model 5616-12, ±0.011°C)

12 in a stable water bath (Fluke 7321).

13

14
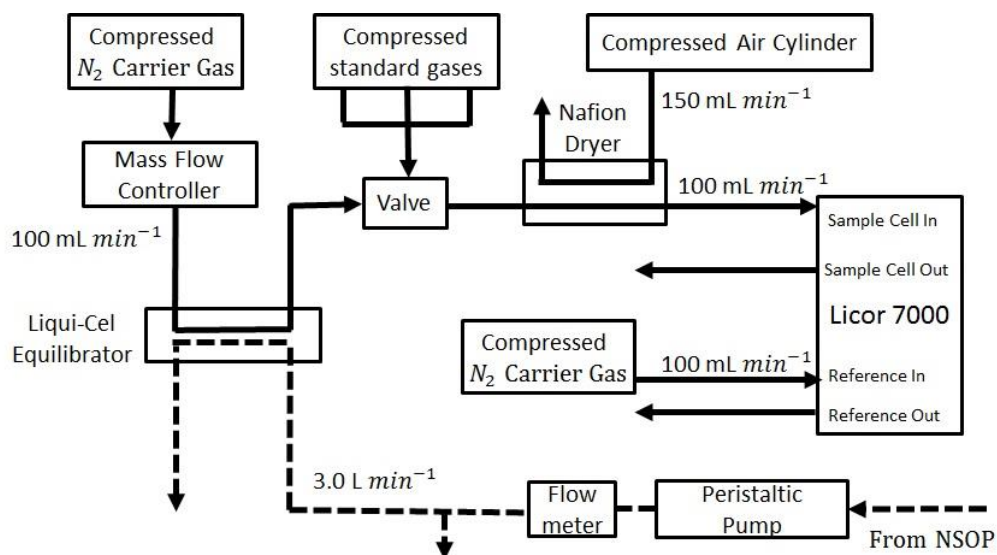
15 **Figure 2:** CO_2 system schematic. Solid and dashed arrows correspond to gas and water flows
16 respectively. The Licor reference cell is flushed with equilibrated gas at 100 ~~ml~~ mL min^{-1}. A
17 manual selection valve was used to switch between equilibrated gas and the CO_2 standards.

18

2.3.1 Equilibrator

The showerhead equilibrator is the most commonly-used equilibrator for CO_2 but takes ~100 s to equilibrate (Dickson et al., 2007; Kitidis et al., 2012; Körtzinger et al., 2000; Webb et al., 2016). This equilibration time is too slow for effective use during NSOP deployments. We used a polypropylene membrane equilibrator (Liqui-Cel, model 2.5x8) with liquid and gas volumes of 0.4 L and 0.15 L and a surface are aof 1.4 m^2. because Due to it' has a large surface area to volume ratio and membrane porosity (50%). t. The Liqui-Cel expedites gas transfer and efficiently achieves equilibration (Loose et al., 2009), with a 3 s response time for CO_2 (Hales et al., 2004). Membrane equilibrators have been used by others for trace gas analysis (Hales et al., 2004; Marandino et al., 2009).

Fugacity of seawater CO_2 is calculated from the Licor gas phase CO_2 measurement. This approach assumes that the gas phase sample has equilibrated fully with the seawater. We performed equilibration efficiency experiments in a seawater tank using a showerhead equilibrator as a reference. Liqui-Cel equilibration efficency declined after prolonged exposure to seawater, likely due to biofouling of the membranes. In a fouled equilibrator, equilibration efficency was a function of the flow rate on both the water and gas side of the membrane. An increased gas flow rate reduces the residence time inside the Liqui-Cel and allows less time to equilibrate (Fig. 3a). Increasing the waterside flow rate moves the gas phase closer to equilibrium because the transfer coefficent in the membrane increases (Fig. 3b).

Cleaning with an acid - base sequence restored the efficiency of a fouled equilibrator. It was necessary to actively pump chemicals through the Liqui-Cel to achieve a full recovery in efficiency. For more details on cleaning techniques, see supplemental material. Efficiency reductions in membrane equilibrators like the Liqui-Cel have not been reported by previous studies. Some authors have used 5-50 µm filters to minimise biofouling (Hales et al., 2004)(Hales et al., 2004) but this was not possible with the NSOP experimental design. If filtering seawater is not possible, we recommend flushing with freshwater after use, regular cleaning of the Liqui-Cel and daily tests to quantify equilibration efficiency. Trace gas measurement systems that use an internal liquid phase standard (e.g. dimethylsulfide, Section 2.4) account for any changes in equilibrator efficiency.
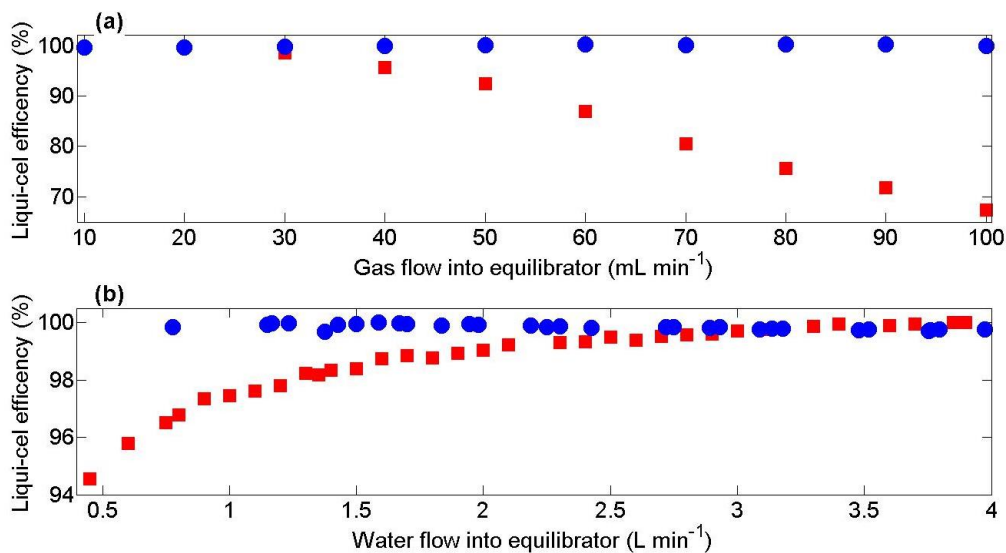
1

Figure 3: Liqui-Cel CO_2 equilibration efficiency (Liqui-Cel mixing ratio / showerhead mixing ratio) for: (a) changing gas flow at a fixed water flow rate of 4 L min^{-1}; and (b) changing water flow at a fixed gas flow of 100 mL min^{-1}. Blue = unfouled equilibrator. Red = fouled equilibrator.

2.4   DMS analysis

DMS was measured with Atmospheric Pressure-Chemical Ionisation Mass Spectrometry (API-CIMS), using a system modified following Saltzman et al. (2009). Measurements were calibrated using an isotopic liquid standard of tri-deuterated DMS ~~(see~~ (see Bell et al., 2013 for details)~~Bell et al., 2013 for details)~~. Isotopic standard was injected at 120 μL min^{-1} into the 3 L min^{-1} seawater flow from NSOP before it entered the Liqui-Cel equilibrator. Compressed nitrogen gas was passed through the equilibrator in the counter direction to the seawater flow at 1 L min^{-1}. The use of an internal standard meant that any incomplete equilibration of the ambient non-isotopic DMS was also true for the isotope. The gas stream exited the equilibrator and was dried (Permapure nafion dryer, model MD-110-48S-4) before entering the mass spectrometer for analysis. DMS was detected at m~~/z (mass~~/charge)~~z~~ 63 and the isotopic standard detected at m/z 66. The concentration of DMS was calculated using the ion signals and relevant flow rates (Bell et al., 2015). This approach has been shown to compare well with other analytical techniques for DMS (Royer et al., 2014; Walker et al., 2016)~~(Walker et al.., 2016; Royer et al., 2014).~~

17

2.5 NSOP ~~response~~ delay and response ~~delay~~ time

We used different approaches to assess the delay between instantaneous miniCTD measurements and water arriving to the ship for analysis. The delay between seawater entering the inlet and reaching the equilibrator was calculated as 114 s using the internal volume of NSOP tubing (0.5 in inner diameter, 54 m length) and a seawater flow rate of 4.15 L min^{-1}. Delay correlation analysis between the NSOP miniCTD temperature sensor and a second sensor positioned at the entrance to the equilibrator gives a similar delay of 112 s. Note that the total delay of the system is greater because it also includes the time that equilibrated gas takes to reach the Licor. We determined the total delay by quickly transferring the seawater inlet quickly between two buckets with distinctly different CO_2 concentrations and timing how long it took for the signal to be detected by the Licor (139 s; Fig. 4).

The response time of the NSOP setup was determined by simulating step changes in gas concentrations. ~~The tubing inlet was quickly transferred between two buckets of seawater with a distinct difference in concentration.~~ A model fit to the exponential change in signal was used to estimate the response time (Fig. 4). We estimate the system response time (e-folding time) for CO_2 as 24 s, which is slightly faster than the 34 s reported by Webb et al. (2016). The e-folding time in the DMS signal is estimated as 11 s, which is consistent with the rapid gas flow rate through the analytical system.

Continuous profiling with the CO_2 system and a 24 s response time yields a depth resolution of 1.2 m, which is greater than the required resolution to assess near surface gradients. DMS has a faster response time than CO_2, but in continuous profiling mode this only translates to a depth resolution of 0.6 m, slightly less than the 1.2-2 m reported by (Royer et al., 2014). A depth resolution of < 0.5 m was desired to capture upper ocean vertical gradients in CO_2 and DMS so NSOP was operated in discrete profiling mode.
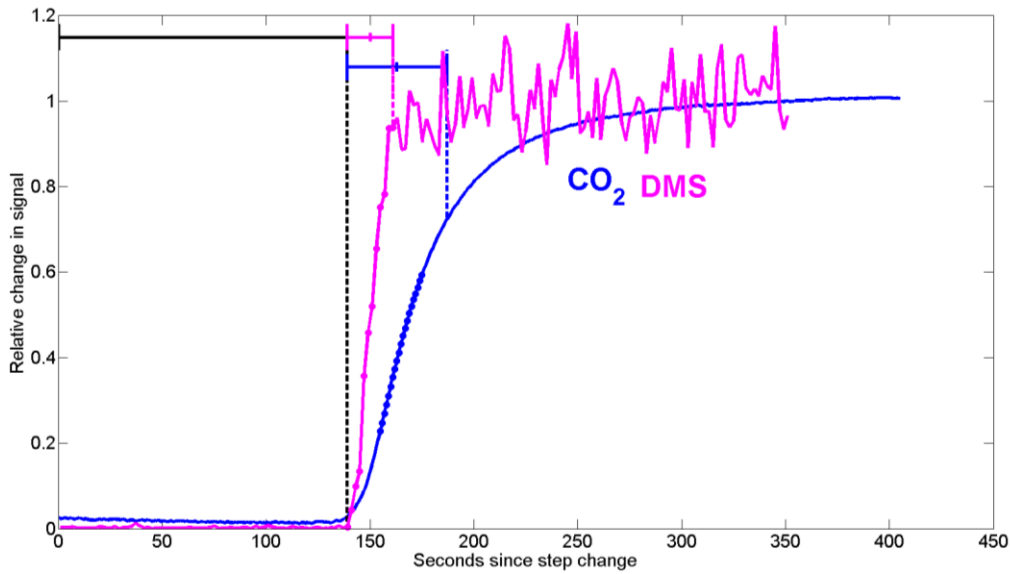
Figure 4: Instrument responses to step changes in seawater CO_2 (blue) and DMS (magenta). Instrument responses have been scaled so that the initial and end concentrations are between 0 and 1. Time is referenced against the point when the step change was initiated. The response is seen in both instruments after a delay of 138 s (black dashed line). Two e-foldings are indicated by vertical dashed lines for CO_2 (blue) and DMS (magenta). The data points marked by circles were used to make an exponential fit to the data to determine the response time (Sect 2.5).

We used different approaches to assess the delay between instantaneous miniCTD measurements and water arriving to the ship for analysis. Using the internal volume of NSOP tubing (0.5 in ID, 54 m length) and a seawater flow rate of 4.15 L min^{-1}, the tubing delay to the equilibrator was calculated as 114 s. Delay correlation analysis between the NSOP miniCTD temperature and a temperature sensor positioned at the entrance to the equilibrator suggests a delay of 112 s. The delay between a bucket switch and a CO_2 change in the Licor was timed at 138 s. The bucket switch delay was longer because the bucket switch experiment also accounts for the delay in the equilibrator and the Licor.

2.6 Data processing

During discrete profiling, distinct sample depths were identified from the rapid changes in pressure during depth transitions. Data were binned into discrete depth bins using CTD

19

1   pressure measurements. Trace gas data were assigned to depth bins after adjusting for the

2   calculated transit time through the NSOP tubing (Section 2.5). CO_2 data from the beginning

3   (2 e-foldings + 15 s buffer = 63 s) and end (15 s buffer) of each depth bin was excluded from

4   analysis to account for the response time of the system and the transition time between sample

5   depths. The same approach was taken for DMS, where the faster response time resulted in a

6   smaller portion of data excluded at the beginning of each depth bin (2 e-foldings + 15 s buffer

7   = 37 s).

8   The CO_2 mixing ratio (xCO_2) measured in the Licor is converted to equilibrator fugacity

9   ($fCO_{2(eq)}$) using calibration standards, *in situ* seawater salinity, and the pressure and

10 temperature in the equilibrator (SOP 5# Underway pCO2 Dickson et al., 2007). Vertical

11 profiles of seawater CO_2 fugacity ($fCO_{2(sw)}$) are calculated using average equilibrator fugacity

12 ($fCO_{2(eq)}$), equilibrator temperature ($T_{(eq)}$) and *in situ* seawater temperature ($T_{(sw)}$) at each

13 depth (Takahashi et al., 1993). ~~The time series $fCO_{2(sw)}$ data shown in (Fig. 7) are also~~

14 ~~calculated using the same equation from Takahashi et al. (1993) but instead use high~~

15 ~~frequency $fCO_{2(sw)}$, $T_{(eq)}$ and $T_{(sw)}$ data.~~

16 **2.7   Seawater sample collection using NSOP**

17 The NSOP setup enables vertical profiles of discrete seawater samples to be collected from

18 upstream of the equilibrator, with a split in the tubing diverting ~0.5 L min^{-1} into a sink. For

19 example, discrete seawater samples (250 ml) have been successfully collected and analysed

20 for Total Alkalinity (TA). Samples were collected and poisoned following best practice

21 recommendations (SOP#1, (Dickson et al., 2007). Bottle filling plus 1 overfill took ~60 s.

22 Start and end times were recorded so that collection depth could be retrospectively

23 determined from the CTD pressure data. Analytical methods and an example depth profile

24 ~~(Fig. S3)~~ are provided in the supplementary information.

25

26 **3   Field Measurements / Observations**

27 Presented below are example profiles collected using NSOP. The first deployment was in the

28 open ocean (July 30th 2015, Central Celtic Sea; 49.4213°N, -8.5783°E) from the *RRS*

29 *Discovery* (100 m length, 6.5 m draught). The second deployment was in coastal waters (15th

30 April 2014, Plymouth Sound; 50.348°N, -4.126°E) from the *RV Plymouth Quest* (20 m

length, 3 m draught). A map of deployment sites is supplied in the supplementary
information.

3.1 Open ocean deployment

NSOP was deployed at 14:05 (UTC) on 30th July 2015. During the 6 hours preceding
deployment, the ship was on station and encountered persistently strong solar radiance (> 600
W m^{-2}), mild winds (< 6 m s^{-1}) and calm sea state (significant wave height < 1.6 m). This
combination of low wind speeds and high irradiance (Fig. S5, supplementary information) is
favourable for near surface stratification (Donlon et al., 2002).
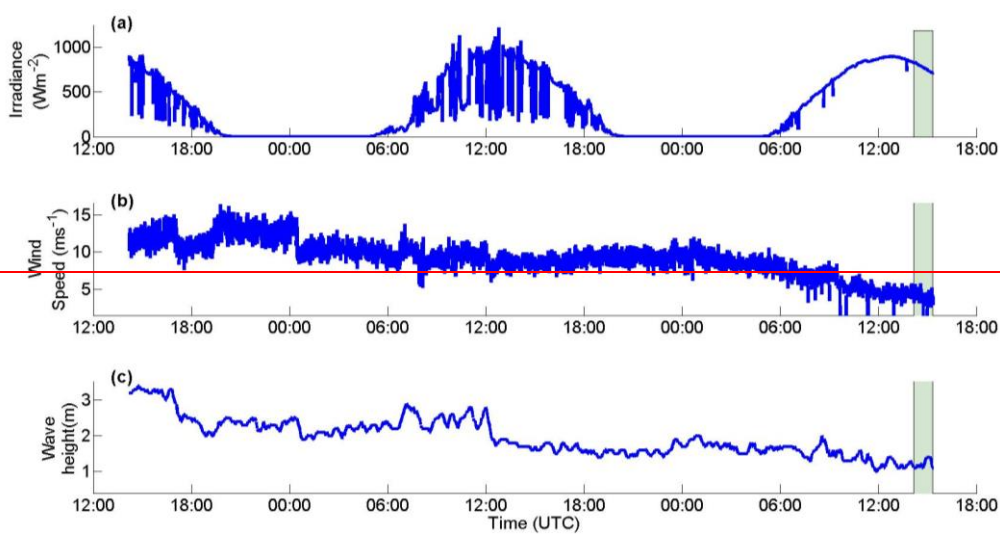
Figure 5: Timeseries of meteorology and sea state variables in the Celtic Cea in July 2015
while the ship was on station: (a) irradiance; (b) wind speed; and (c) significant wave height.
The data begin 48 h before the start of the profile at 14:05 hrs (UTC). The vertical grey bar
indicates the period when NSOP was profiling.

Fig. 6 5 presents the time series data collected by NSOP for depth, temperature, salinity and
$fCO_{2(sw)}$. Discrete profiling began at 14:05 hrs (UTC) at 0.7 m depth, which was as close to
the surface as the frame could be located without the possibility of breaking the surface.
Depth bins were identified based on rapid depth transitions (Fig. 6a5a). Bottles were filled for
discrete samples during the downcast. Profiling lasted 75 minutes and finished back at the
surface at 15:20 hrs (UTC). Seawater temperature was 16.61± 0.06 °C. At 14:20 hrs (UTC)
$fCO_{2(atm)}$ was 398 µatm and$fCO_{2(sw)}$ was 389 µatm at 0.67 mSeawater temperature was 16.61±

1   ~~0.06 °C and fCO~~$_{2(sw)}$ ~~was~~meaning the ocean was undersaturated with respect to the

2   atmosphere.~~.~~ The temeperature and seawater CO$_2$~~both~~ were the expected magnitude for

3   summer in the Celtic Sea (Frankignoulle and Borges, 2001). Salinity was homogeneous

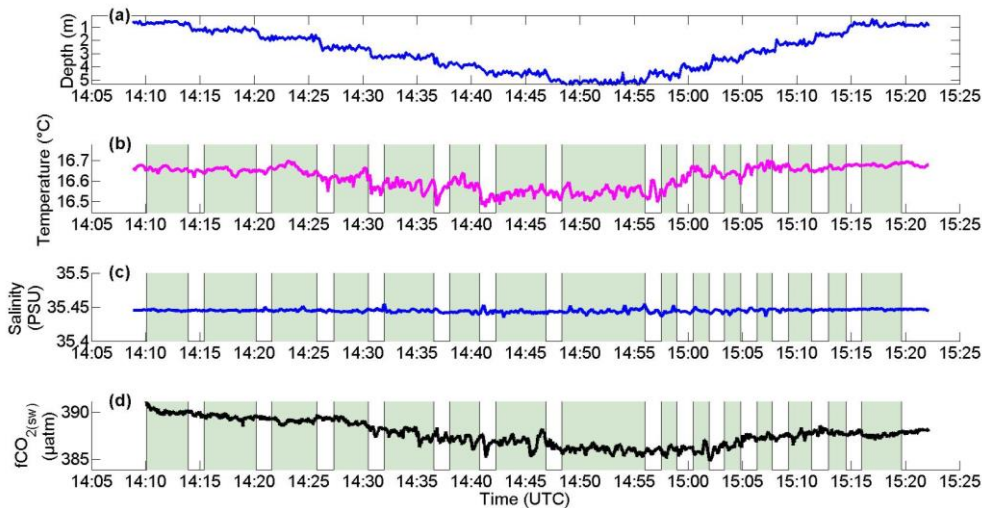4   throughout the NSOP deployment, only varying by ±0.004.

5

6   **Figure ~~6~~5:** Time series measurements made during an NSOP deployment in the Celtic Sea on
7   30th July 2015. Data are 1 Hz depth (a), seawater temperature (b), salinity (c) and fCO$_{2(sw)}$ (d).
8   Data used for depth bin analysis (Section 2.6) is identified by a shaded background.

9

10 Depth-binned salinity and temperature data did not show any significant variability (Fig.

11 ~~7a~~6a). A slight temperature gradient was observed, with 0.15°C difference between 5 m and

12 the surface and a fairly constant reduction with depth (0.03°C per metre). The temperature

13 profile was similar for down and up casts, although some continued warming of surface

14 waters was evident in the up cast. The temperature measured by NSOP at 5.15 m depth agrees

15 well with the coincident temperature measured by the bow thermistor at 5.5 m (< 0.02°C

16 difference) (Fig. ~~7c~~6c). There is no evidence that the ship's thrusters/propellers disrupted the

17 near surface gradients.

18 We compare the NSOP temperature profile with thermistor readings from a series of Sea-Bird

19 Sc~~e~~ientific (SBE 56) sensors (0.3, 0.6, 1.5, 3.5 and 7 m depth) mounted on a nearby

20 temperature chain moor~~ed~~ing ~2.8 km away (49.403°N, -8.606°E) ~~from the deployment site~~

21 ~~(0.3, 0.6, 1.5, 3.5 and 7 m depth)~~. The vertical profile implied by the NSOP deployment

22 agrees with the mooring data (Fig. ~~7c~~6c), and corroborates the warming of the upper few

1 metres of the ocean observed during the deployment. The agreement between these

2 independent datasets suggests that it is unlikely that NSOP caused any significant localized

3 warming of surface waters. The mean difference between NSOP temperature from discrete

4 depths and the mooring sensors is 0.02°C. The surface data from the NSOP up cast show less

5 agreement with the mooring, with NSOP temperatures ~0.05 °C lower than the 0.3 m and 0.6

6 m mooring sensors. During the profile the ship drifted ~1 km from the start position of the

7 profile and a further 0.2 km from the mooring. The small offset between the NSOP surface

8 temperatures and the mooring may be driven by horizontal variability between the

9 deployment and mooring locations. It is also possible that turbulence mixed warm surface

10 waters down into cooler sub-surface layers. Turbulence could have been generated around the

11 NSOP sampling frame or by an increase in wave-driven mixing when the significant wave

12 height increased at ~15:00 hrs UTC (Fig. 5AS4a).

13
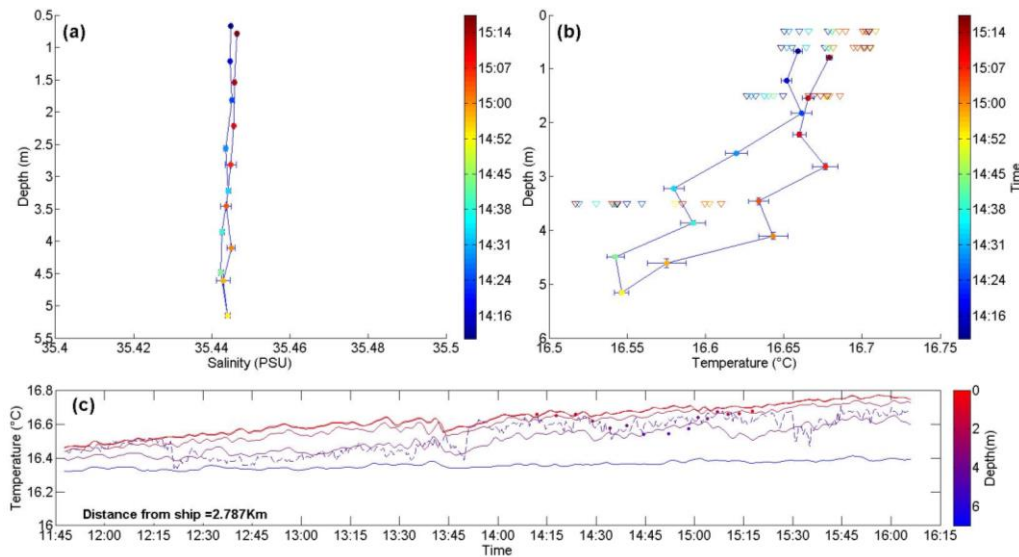
14 **Figure 76:** Salinity and temperature in the Central Celtic Sea on 30th July 2015. NSOP
15 profiles of salinity (a) and temperature (b) were derived using depth bins as described in
16 Section 2.6. Data points are coloured by sampling time. Vertical and horizontal error bars
17 show two standard errors of the mean in each depth bin. Coloured triangles in (B) are time-
18 averaged temperature for four depths (0.3, 0.6, 1.5 and 3.5 m) at the nearby Central Celtic Sea
19 temperature mooring (49.403°N, -8.606°E). (c) Timeseries of temperature at the mooring.
20 Timeseries of temperature at depths (0.3, 0.6, 1.5 and 3.5 m) are solid lines whereas the
21 dDashed line is the underway temperature at 5.5 m from *RRS Discovery* (located 2.8 km from
22 the mooring). The mooring and underway temperatures are coloured according to their sample
23 depth, where red is the air/sea interface. The Coloured circles are binned temperature data

1 from NSOP which have also been coloured to reflect the depth of collection. ~~Sample depth is~~
2 ~~indicated by blue-red colour, where red is the air/sea interface.~~

3

4 Seawater density (Fig. ~~8a~~7a) was calculated using the salinity and temperature profile data
5 (Fig. ~~7a~~6a &~~7b~~6b) and the 1983 Unesco equation of state (Millero and Poisson, 1981). As
6 expected with little variation in the salinity, changes in the density profile are dominated by
7 temperature. The down and up casts for CO_2 show excellent agreement below 2.5 m. Surface
8 water (< 2 m) CO_2 is 2-4 µatm higher than at 5 m (Fig. ~~8b~~7b). Elevated surface CO_2 could be
9 explained by a sustained flux from the atmosphere into a near surface stratified layer with
10 inhibited deep water exchange. Under this assumption a vertical gradient in seawater CO_2
11 would need to be established shortly after the temperature gradient. A paired t-test showed
12 that thefCO$_2$ measured in the surface bins on the downcast and upcast are were significantly
13 different (p = <0.001) ~~Surface CO$_2$ is significantly different between the down and up casts~~.
14 The deepening of the surface stratified layer could explain the more homogeneous CO_2 during
15 the upcast. It is worth noting that in addition to physical processes, plankton trapped within
16 the surface layer could also modify the surface CO_2. Trace gas concentrations may also be
17 different in the sea surface microlayer but sampling that close to the surface is beyond the
18 capabilities of NSOP. Complimentary measurements of the sea surface microlayer could be
19 made using other state of the art purpose built sampling platforms such as the Sea Surface
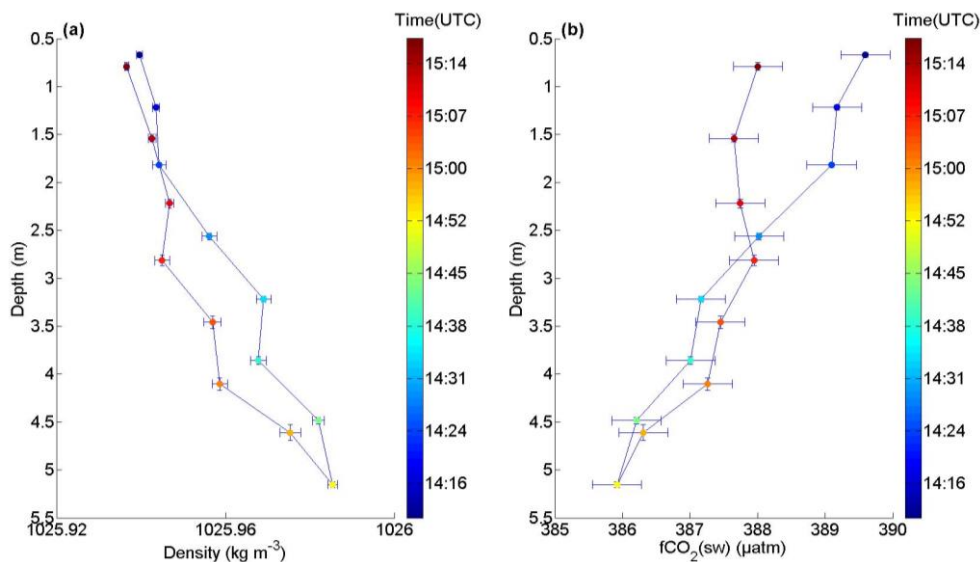20 Scanner (Ribas-Ribas et al., 2017).

21

1 **Figure 8̶7:** NSOP density (a) and $fCO_{2(sw)}$ (b) profiles from the Celtic Sea on 30th July 2015.
2 Data points are coloured by sample time. Vertical error bars correspond to two standard
3 errors of the mean in each depth bin. The horizontal error bars in (a) are two standard errors of
4 the mean, whereas in (b) they are the propogated error from the the binned measurements used
5 to calculate $fCO_{2(sw)}$.

6

7 To assess measurement accuracy the NSOP Liqui-Cel CO_2 system was compared against an

8 independent CO_2 system that had a showerhead equilibrator coupled to the ship's seawater

9 supply pumped from 5.5 m below the sea surface (Hardman-Mountford et al., 2008; Kitidis et

10 al., 2012). Technical issues meant that the underway CO_2 system installed on the *RRS*

11 *Discovery* was not functioning during the deployment detailed above. However during a

12 deployment on the 19th July 2015, the $fCO_{2(sw)}$ measured by NSOP at 5 m agreed well with

13 independent measurements from the underway system, difference = 1.7+/- 4.18 µatm. The

14 agreement between the two systems is in line with previous intercomparisons(Royer et al.,

15 2016; Ribas-Ribas et al., 2014)(Ribas-Ribas et al., 2014; Körtzinger et al., 2000). However

16 during deployments on the 19th and 20th July, the $fCO_{2(sw)}$ measured by NSOP close to the

17 underway intake depth agrees to within 3 µatm.

18

19 **3.2 Coastal deployment**

20 DMS profiles were collected on a small research vessel on 15th April 2014. NSOP was

21 deployed within the Plymouth Sound at 12:00 hrs UTC and recovered 95 minutes later (Fig.

22 1̶08). In the sheltered environment behind the breakwater the standard deviation in depth was

23 ±0.10 m, smaller than observed during open ocean profiles. Seawater temperature and salinity

24 demonstrate clear structure, with lower temperatures and higher salinities associated with sub-

25 surface water. Two river estuaries (Plym and Tamar) converge and flow out to the open ocean

26 through the Plymouth Sound. We likely observed a freshwater surface lens that was protected

27 from wave-driven mixing and had been warmed over the course of the day. We used a

28 different miniCTD during this deployment and were thus also able to collect fluorescence

29 data (Fig. 1̶0̶d8d).

30 Temperature profiles (Fig. 1̶1̶a9a) show a sharp discontinuity in the downcast at ~5 m

31 whereas in the upcast the thermocline had shoaled to ~3.5 m. The salinity profiles suggest

32 similar mixing depths to the temperature profiles, with lower salinity water at the surface (Fig.

1   10b9b). Fluorescence increases with depth (Fig. 10c9c), but this is likely due to quenching of

2   the phytoplankton photosynthetic apparatus at the surface(Smyth et al., 2004). DMS

3   concentrations reduce steadily with depth (Fig. 10d9d), which is likely explained by changes

4   in DMS production and consumption rates by the biological community (Galí et al., 2013).

5   The DMS profiles from the upcast and the downcast are very similar, with the largest

6   difference at the very surface. A large difference in the surface-most data point can also be

7   seen in the temperature data, and may reflect mixing with sub-surface waters due to the

8   motion of NSOP or short time-scale variations in the physical environment.
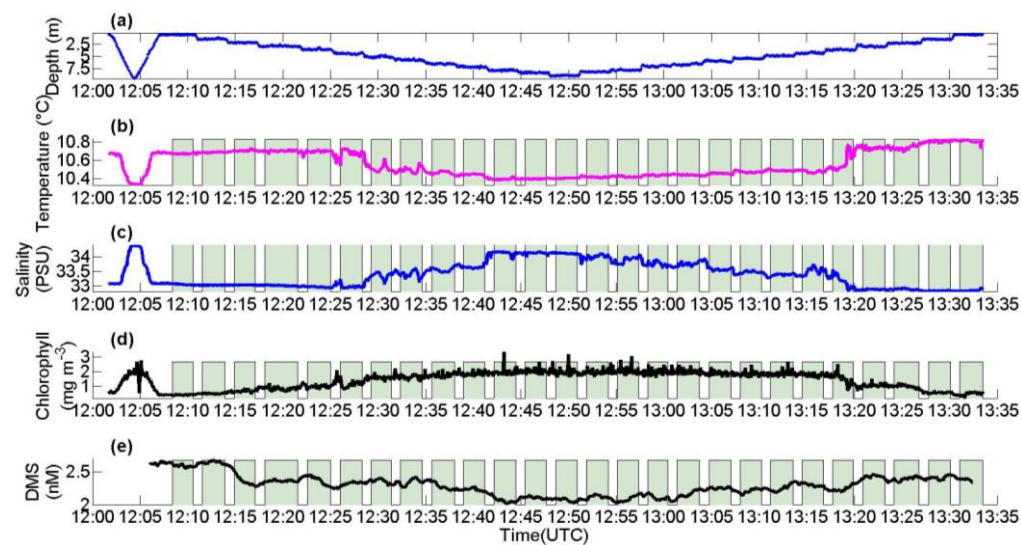
Figure 98: Time series measurements during an NSOP deployment in Plymouth Sound on
15th April 2014: depth (a), temperature (b), salinity (c), chlorophyll fluorescence (d) and
$DMS_{(sw)}$ (e). Data used for depth bin analysis (Section 2.6) is identified by a shaded
background. The beginning of the time series is an example off a continuous profile (see
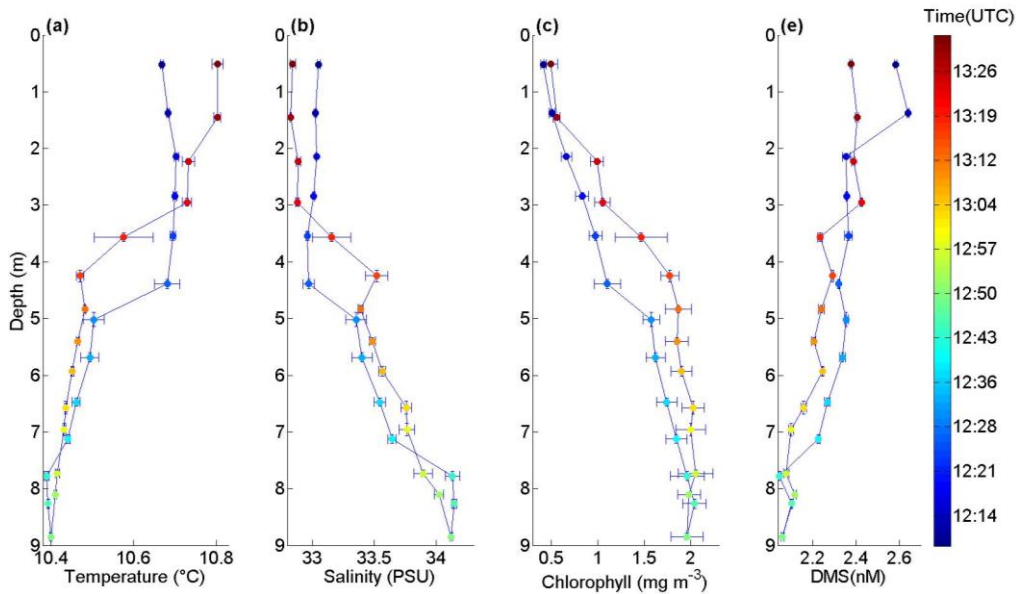Section 2.2).

Figure 109: NSOP profiles collected in Plymouth Sound on 15th April 2014: temperature (a), salinity (b), chlorophyll fluorescence (c), and $DMS_{(sw)}$ (d). Data are coloured by sample time. Vertical and horizontal error bars are two standard errors of the mean (SEM) in each depth bin.

4   Summary

This paper describes a Near Surface Ocean Profiler (NSOP) designed to measure vertical trace gas profiles near the air-sea interface. NSOP is unique in approach as its sampling frame is lowered from a buoy that rides the ocean swell, reducing relative motion of the frame and hence fluctuations in sampling depth. The NSOP design facilitates near surface (< 0.5 m) sampling, significantly improving the capability to resolve vertical gradients. Other benefits include the ability to sample away from ship-driven turbulence and the flexibility to make a large range of near surface measurements. The NSOP sampling frame houses the miniCTD and also has the capacity to incorporate additional sensors (e.g. turbulence, dissolved oxygen and other measures of phytoplankton abundance and photosynthetic health). The ability to collect water from discrete depths facilitates the collection of near surface samples that require additional processing or take longer to analyse (e.g. TA, dissolved inorganic carbon, nutrients, the DMS-precursor DMSP, dissolved organic carbon). NSOP is highly versatile and can be used for continuous or discrete profiling. Further development could adjust winch pay

out speed and enable continuous, high resolution depth profiles for slower response time measurements (e.g. $fCO_{2(sw)}$).

Near surface stratification in the upper few metres of the ocean due to temperature and salinity gradients is a well-documented phenomenon. The presence or absence of chemical and biological gradients within near surface stratified layers has been difficult to assess. NSOP is a platform with the capability to successfully resolve gradients in these near surface layers. The data presented in this paper demonstrate that near surface gradients in trace gases can lead to substantially different fluxes depending upon the seawater depth that is used to calculate the flux. Assuming that the effect of temperature and salinity gradients on the flux can be accounted for using remote sensing methods (e.g Shutler et al., 2016), then the change in flux is directly proportional to the change in ΔC. In the case of the coastal DMS profile, a higher concentration (2.6 nM) was observed 0.5 m below the sea surface compared to concentrations at 5 m (2.4 nM). Assuming that the atmospheric concentration of DMS was zero (a typical approach for DMS fluxes, (see Lana et al., 2011)this will result in a corresponding flux increase of 10 %. In the case of the Celtic Sea CO_2 profile, the concentration at 0.5 m (389.6 µatm) was higher than at 5 m (385.9 µatm). The atmospheric CO_2 concentration was 398.1 µatm, which means that the surface water was less undersaturated than implied by the seawater concentration at 5 m. Thus the ΔC and calculated air-to-sea flux are lower by 30%. The magnitude of these concentration gradients are significant, but it is unlikely that the gradients we observed will persist for all hours of the day, under different environmental conditions and in all regions of the global ocean. A subsequent publication is planned that discusses four cruises where NSOP was deployed as well as the wider prevalence and implications of near surface CO_2 gradients.

Near surface stratification in the upper few metres of the ocean due to temperature and salinity gradients is a well-documented phenomenon. The presence or absence of chemical and biological gradients within near surface stratified layers has been difficult to assess. NSOP is a platform with the capability to successfully resolve gradients in these near surface layers.

28

8

9   References

10 Bakker, D. C., Pfeil, B., Landa, C. S., Metzl, N., O'brien, K. M., Olsen, A., Smith, K., Cosca,
11 C., Harasawa, S., and Jones, S. D.: A multi-decade record of high-quality fCO 2 data in
12 version 3 of the Surface Ocean CO 2 Atlas (SOCAT), Earth System Science Data, 8, 383,
13 2016.

14 Bange, H. W., Bell, T. G., Cornejo, M., Freing, A., Uher, G., Upstill-Goddard, R. C., and
15 Zhang, G.: MEMENTO: a proposal to develop a database of marine nitrous oxide and
16 methane measurements, Environmental Chemistry, 6, 195-197, 2009.

17 Bell, T., De Bruyn, W., Miller, S., Ward, B., Christensen, K., and Saltzman, E.: Air–sea
18 dimethylsulfide (DMS) gas transfer in the North Atlantic: evidence for limited interfacial gas
19 exchange at high wind speed, Atmospheric Chemistry and Physics, 13, 11073-11087, 2013.

20 Bell, T., De Bruyn, W., Marandino, C. A., Miller, S., Law, C., Smith, M., and Saltzman, E.:
21 Dimethylsulfide gas transfer coefficients from algal blooms in the Southern Ocean,
22 Atmospheric Chemistry and Physics, 15, 1783-1794, 2015.

23 Dickson, A. G., Sabine, C. L., and Christian, J. R.: Guide to best practices for ocean CO_2
24 measurements, 2007.

25 Donlon, C., Minnett, P., Gentemann, C., Nightingale, T., Barton, I., Ward, B., and Murray,
26 M.: Toward improved validation of satellite sea surface skin temperature measurements for
27 climate research, Journal of Climate, 15, 353-369, 2002.

28 Durham, W. M., Kessler, J. O., and Stocker, R.: Disruption of vertical motility by shear
29 triggers formation of thin phytoplankton layers, Science, 323, 1067-1070, 2009.

30 Fairall, C., Bradley, E. F., Godfrey, J., Wick, G., Edson, J. B., and Young, G.: Cool-skin and
31 warm-layer effects on sea surface temperature, Journal of Geophysical Research, 101, 1295-
32 1308, 1996.

33 Frankignoulle, M., and Borges, A. V.: European continental shelf as a significant sink for
34 atmospheric carbon dioxide, Global Biogeochemical Cycles, 15, 569-576, 2001.

35 Galí, M., Simó, R., Vila-Costa, M., Ruiz-González, C., Gasol, J. M., and Matrai, P.: Diel
36 patterns of oceanic dimethylsulfide (DMS) cycling: Microbial and physical drivers, Global
37 Biogeochemical Cycles, 27, 620-636, 2013.

Hales, B., Chipman, D., and Takahashi, T.: High-frequency measurement of partial pressure and total concentration of carbon dioxide in seawater using microporous hydrophobic membrane contractors, Limnol. Oceanogr.: Methods 2, 356-364, 2004.

Hardman-Mountford, N. J., Moore, G., Bakker, D. C., Watson, A. J., Schuster, U., Barciela, R., Hines, A., Moncoiffé, G., Brown, J., and Dye, S.: An operational monitoring system to provide indicators of CO_2-related variables in the ocean, ICES Journal of Marine Science: Journal du Conseil, 65, 1498-1503, 2008.

Kitidis, V., Hardman-Mountford, N. J., Litt, E., Brown, I., Cummings, D., Hartman, S., Hydes, D., Fishwick, J. R., Harris, C., and Martinez-Vicente, V.: Seasonal dynamics of the carbonate system in the Western English Channel, Continental Shelf Research, 42, 30-40, 2012.

Körtzinger, A., Mintrop, L., Wallace, D. W., Johnson, K. M., Neill, C., Tilbrook, B., Towler, P., Inoue, H. Y., Ishii, M., and Shaffer, G.: The international at-sea intercomparison of fCO_2 systems during the R/V Meteor Cruise 36/1 in the North Atlantic Ocean, Marine Chemistry, 72, 171-192, 2000.

Lana, A., Bell, T., Simó, R., Vallina, S. M., Ballabrera-Poy, J., Kettle, A., Dachs, J., Bopp, L., Saltzman, E., and Stefels, J.: An updated climatology of surface dimethlysulfide concentrations and emission fluxes in the global ocean, Global Biogeochemical Cycles, 25, 2011.

Le Quéré, C., Andrew, R. M., Canadell, J. G., Sitch, S., Korsbakken, J. I., Peters, G. P., Manning, A. C., Boden, T. A., Tans, P. P., and Houghton, R. A.: Global carbon budget 2016, Earth System Science Data, 8, 605, 2016.

Liss, P. S., and Slater, P. G.: Flux of Gases across the Air-Sea Interface, Nature, 247, 181-184, 1974.

Loose, B., Stute, M., Alexander, P., and Smethie, W.: Design and deployment of a portable membrane equilibrator for sampling aqueous dissolved gases, Water Resources Research, 45, 2009.

Marandino, C. A., De Bruyn, W. J., Miller, S. D., and Saltzman, E. S.: Open ocean DMS air/sea fluxes over the eastern South Pacific Ocean, Atmos. Chem. Phys., 9, 345-356, 10.5194/acp-9-345-2009, 2009.

McNeil, C. L., and Merlivat, L.: The warm oceanic surface layer: Implications for CO_2 fluxes and surface gas measurements, Geophysical research letters, 23, 3575-3578, 1996.

Miller, S. D., Marandino, C., and Saltzman, E. S.: Ship-based measurement of air-sea CO_2 exchange by eddy covariance, Journal of Geophysical Research: Atmospheres, 115, 2010.

Millero, F. J., and Poisson, A.: International one-atmosphere equation of state of seawater, Deep Sea Research Part A. Oceanographic Research Papers, 28, 625-629, 1981.

Quinn, P., and Bates, T.: The case against climate regulation via oceanic phytoplankton sulphur emissions, Nature, 480, 51-56, 2011.

Ribas-Ribas, M., Rerolle, V., Bakker, D. C., Kitidis, V., Lee, G., Brown, I., Achterberg, E. P., Hardman-Mountford, N., and Tyrrell, T.: Intercomparison of carbonate chemistry measurements on a cruise in northwestern European shelf seas, Biogeosciences, 11, 4339-4355, 2014.

Ribas-Ribas, M., Mustaffa, N. I. H., Rahlff, J., Stolle, C., and Wurl, O.: Sea Surface Scanner (S3): A Catamaran for High-resolution Measurements of Biogeochemical Properties of the Sea Surface Microlayer, Journal of Atmospheric and Oceanic Technology, 2017.

Robertson, J. E., and Watson, A. J.: Thermal skin effect of the surface ocean and its implications for CO_2 uptake, Nature, 358, 738-740, 1992.

Royer, S.-J., Galí, M., Saltzman, E. S., McCormick, C. A., Bell, T. G., and Simó, R.: Development and validation of a shipboard system for measuring high-resolution vertical profiles of aqueous dimethylsulfide concentrations using chemical ionisation mass spectrometry, Environmental Chemistry, 11, 309-317, 2014.

Royer, S. J., Galí, M., Mahajan, A. S., Ross, O. N., Pérez, G. L., Saltzman, E. S., and Simó, R.: A high-resolution time-depth view of dimethylsulphide cycling in the surface sea, Scientific Reports, 6, 32325, 2016.

Saltzman, E. S., De Bruyn, W. J., Lawler, M., Marandino, C., and McCormick, C.: A chemical ionization mass spectrometer for continuous underway shipboard analysis of dimethylsulfide in near-surface seawater, Ocean Science, 5, 537-546, 2009.

Shutler, J. D., Land, P. E., Piolle, J.-F., Woolf, D. K., Goddijn-Murphy, L., Paul, F., Girard-Ardhuin, F., Chapron, B., and Donlon, C. J.: FluxEngine: A Flexible Processing System for Calculating Atmosphere–Ocean Carbon Dioxide Gas Fluxes and Climatologies, Journal of Atmospheric and Oceanic Technology, 33, 741-756, 2016.

Smyth, T., Pemberton, K., Aiken, J., and Geider, R.: A methodology to determine primary production and phytoplankton photosynthetic parameters from fast repetition rate fluorometry, Journal of Plankton Research, 26, 1337-1350, 2004.

Smyth, T. J., Fishwick, J. R., Lisa, A.-M., Cummings, D. G., Harris, C., Kitidis, V., Rees, A., Martinez-Vicente, V., and Woodward, E. M.: A broad spatio-temporal view of the Western English Channel observatory, Journal of Plankton Research, 32, 585-601, 2010.

Takahashi, T., Olafsson, J., Goddard, J. G., Chipman, D. W., and Sutherland, S.: Seasonal variation of CO_2 and nutrients in the high-latitude surface oceans: A comparative study, Global Biogeochemical Cycles, 7, 843-878, 1993.

Turk, D., Zappa, C. J., Meinen, C. S., Christian, J. R., Ho, D. T., Dickson, A. G., and McGillis, W. R.: Rain impacts on CO_2 exchange in the western equatorial Pacific Ocean, Geophysical Research Letters, 37, 2010.

Walker, C. F., Harvey, M. J., Smith, M. J., Bell, T. G., Saltzman, E. S., Marriner, A. S., McGregor, J. A., and Law, C. S.: Assessing the potential for dimethylsulfide enrichment at the sea surface and its influence on air-sea flux, Ocean Science, 12, 1033, 2016.

Wanninkhof, R.: Relationship between wind speed and gas exchange over the ocean revisited, Limnol. Oceanogr. Methods, 12, 351-362, 2014.

Ward, B., Wanninkhof, R., McGillis, W. R., Jessup, A. T., DeGrandpre, M. D., Hare, J. E., and Edson, J. B.: Biases in the air-sea flux of CO_2 resulting from ocean surface temperature gradients, Journal of Geophysical Research: Oceans (1978–2012), 109, 2004.

Webb, J. R., Maher, D. T., and Santos, I. R.: Automated, in situ measurements of dissolved CO_2, CH_4, and $\delta 13C$ values using cavity enhanced laser absorption spectrometry: Comparing response times of air-water equilibrators, Limnology and Oceanography: Methods, 14, 323-337, 2016.

1 Woolf, D., Land, P. E., Shutler, J. D., Goddijn-Murphy, L., and Donlon, C. J.: On the
2 calculation of air-sea fluxes of CO_2 in the presence of temperature and salinity gradients,
3 Journal of Geophysical Research: Oceans, 2016.

4 Yang, M., Beale, R., Smyth, T., and Blomquist, B.: Measurements of OVOC fluxes by eddy
5 covariance using a proton-transfer-reaction mass spectrometer–method development at a
6 coastal site, Atmospheric Chemistry and Physics, 13, 6165-6184, 2013.

7 Ziska, F., Quack, B., Abrahamsson, K., Archer, S., Atlas, E., Bell, T., Butler, J., Carpenter,
8 L., Jones, C., and Harris, N.: Global sea-to-air flux climatology for bromoform,
9 dibromomethane and methyl iodide, Atmospheric Chemistry and Physics, 13, 8915-8934,
10 2013.

11

12